Measurement of Double-Polarization Asymmetries in the Quasielastic $^{3}\overrightarrow{\mathrm{He}}(\vec{e},e'd)$ Process

M. Mihovilovič,[1,†] G. Jin,[2] E. Long,[3] Y.-W. Zhang,[4] K. Allada,[5] B. Anderson,[3] J. R. M. Annand,[6] T. Averett,[7] W. Boeglin,[8] P. Bradshaw,[7] A. Camsonne,[5] M. Canan,[9] G. D. Cates,[2] C. Chen,[10] J. P. Chen,[5] E. Chudakov,[5] R. De Leo,[11] X. Deng,[2] A. Deltuva,[12,13] A. Deur,[5] C. Dutta,[14] L. El Fassi,[4] D. Flay,[15] S. Frullani,[16] F. Garibaldi,[16] H. Gao,[17] S. Gilad,[18] R. Gilman,[4] O. Glamazdin,[19] J. Golak,[20] S. Golge,[9] J. Gomez,[5] O. Hansen,[5] D. W. Higinbotham,[5] T. Holmstrom,[21] J. Huang,[18] H. Ibrahim,[22] C. W. de Jager,[5] E. Jensen,[23] X. Jiang,[24] M. Jones,[5] H. Kang,[25] J. Katich,[7] H. P. Khanal,[8] A. Kievsky,[26] P. King,[27] W. Korsch,[14] J. LeRose,[5] R. Lindgren,[2] H.-J. Lu,[28] W. Luo,[29] L. E. Marcucci,[30] P. Markowitz,[8] M. Meziane,[7] R. Michaels,[5] B. Moffit,[5] P. Monaghan,[10] N. Muangma,[18] S. Nanda,[5] B. E. Norum,[2] K. Pan,[18] D. Parno,[31] E. Piasetzky,[32] M. Posik,[15] V. Punjabi,[33] A. J. R. Puckett,[24] X. Qian,[17] Y. Qiang,[5] X. Qui,[29] S. Riordan,[2] A. Saha,[5,*] P. U. Sauer,[34] B. Sawatzky,[5] R. Schiavilla,[5,9] B. Schoenrock,[35] M. Shabestari,[2] A. Shahinyan,[36] S. Širca,[39,1,‡] R. Skibiński,[20] J. St. John,[21] R. Subedi,[37] V. Sulkosky,[18] W. A. Tobias,[2] W. Tireman,[35] G. M. Urciuoli,[16] M. Viviani,[26] D. Wang,[2] K. Wang,[2] Y. Wang,[38] J. Watson,[5] B. Wojtsekhowski,[5] H. Witała,[20] Z. Ye,[10] X. Zhan,[18] Y. Zhang,[29] X. Zheng,[2] B. Zhao,[7] and L. Zhu[10]

(Jefferson Lab Hall A Collaboration)

[1]*Jožef Stefan Institute, SI-1000 Ljubljana, Slovenia*
[2]*University of Virginia, Charlottesville, Virginia 22908, USA*
[3]*Kent State University, Kent, Ohio 44242, USA*
[4]*Rutgers University, New Brunswick, New Jersey 08901, USA*
[5]*Thomas Jefferson National Accelerator Facility, Newport News, Virginia 23606, USA*
[6]*Glasgow University, Glasgow G12 8QQ, Scotland, United Kingdom*
[7]*The College of William and Mary, Williamsburg, Virginia 23187, USA*
[8]*Florida International University, Miami, Florida 33181, USA*
[9]*Old Dominion University, Norfolk, Virginia 23529, USA*
[10]*Hampton University, Hampton, Virginia 23669, USA*
[11]*Università degli studi di Bari Aldo Moro, I-70121 Bari, Italy*
[12]*Center for Nuclear Physics, University of Lisbon, P-1649-003 Lisbon, Portugal*
[13]*Institute for Theoretical Physics and Astronomy, Vilnius University, LT-01108 Vilnius, Lithuania*
[14]*University of Kentucky, Lexington, Kentucky 40506, USA*
[15]*Temple University, Philadelphia, Pennsylvania 19122, USA*
[16]*Istituto Nazionale Di Fisica Nucleare, INFN/Sanita, Roma, Italy*
[17]*Duke University, Durham, North Carolina 27708, USA*
[18]*Massachusetts Institute of Technology, Cambridge, Massachusetts 02139, USA*
[19]*Kharkov Institute of Physics and Technology, Kharkov 61108, Ukraine*
[20]*M. Smoluchowski Institute of Physics, Jagiellonian University, PL-30059 Kraków, Poland*
[21]*Longwood College, Farmville, Virginia 23909, USA*
[22]*Cairo University, Cairo, Giza 12613, Egypt*
[23]*Christopher Newport University, Newport News, Virginia 23606, USA*
[24]*Los Alamos National Laboratory, Los Alamos, New Mexico 87545, USA*
[25]*Seoul National University, Seoul, Korea*
[26]*INFN-Pisa, I-56127 Pisa, Italy*
[27]*Ohio University, Athens, Ohio 45701, USA*
[28]*Huangshan University, People's Republic of China*
[29]*Lanzhou University, Lanzhou, Gansu, 730000, People's Republic of China*
[30]*Physics Department, Pisa University, I-56127 Pisa, Italy*
[31]*Carnegie Mellon University, Pittsburgh, Pennsylvania 15213, USA*
[32]*Tel Aviv University, Tel Aviv 69978, Israel*
[33]*Norfolk State University, Norfolk, Virginia 23504, USA*
[34]*Institute for Theoretical Physics, University of Hannover, D-30167 Hannover, Germany*
[35]*Northern Michigan University, Marquette, Michigan 49855, USA*
[36]*Yerevan Physics Institute, Yerevan, Armenia*
[37]*George Washington University, Washington, D.C. 20052, USA*
[38]*University of Illinois at Urbana-Champaign, Urbana, Illinois 61801, USA*
[39]*University of Ljubljana, SI-1000 Ljubljana, Slovenia*
(Received 11 September 2014; published 5 December 2014)

We present a precise measurement of double-polarization asymmetries in the $^3\overrightarrow{\mathrm{He}}(\vec{\mathrm{e}}, e'd)$ reaction. This particular process is a uniquely sensitive probe of hadron dynamics in ^{3}He and the structure of the underlying electromagnetic currents. The measurements have been performed in and around quasielastic kinematics at $Q^2 = 0.25(\mathrm{GeV}/c)^2$ for missing momenta up to 270 MeV$/c$. The asymmetries are in fair agreement with the state-of-the-art calculations in terms of their functional dependencies on p_m and ω, but are systematically offset. Beyond the region of the quasielastic peak, the discrepancies become even more pronounced. Thus, our measurements have been able to reveal deficiencies in the most sophisticated calculations of the three-body nuclear system, and indicate that further refinement in the treatment of their two-and/or three-body dynamics is required.

DOI: 10.1103/PhysRevLett.113.232505 PACS numbers: 21.45.-v, 25.30.-c, 27.10.+h

The ^{3}He nucleus lies at the very heart of nuclear physics and, along with the deuteron, represents the perfect playground to test nuclear dynamics (see, for example, [1–3] and references therein). The understanding of its structure has far-reaching implications not only for nuclear physics itself, but also for a variety of ^{3}He-based experiments seeking to extract the neutron information by exploiting ^{3}He as an effective neutron target. These extractions rely on a virtually perfect theoretical knowledge of the ground-state spin structure of ^{3}He. In particular, the statistical precision of double-polarization experiments on ^{3}He has become comparable to the systematic uncertainty implied by our imperfect knowledge of the polarization of the protons and the neutron within the polarized ^{3}He nucleus. This increase in precision needs to be matched by the best theoretical models which, in turn, require increasingly accurate input to adjust their parameters, complete understanding of the spin and isospin dependence of the reaction-mechanism effects such as final-state interactions (FSI) and meson-exchange currents (MEC), as well as an evaluation of the possible role of three-nucleon forces.

The most fruitful approach to studying the ^{3}He nucleus is by electron-induced knockout of protons, neutrons, and deuterons. In this Letter we focus on the deuteron channel. In the $^3\overrightarrow{\mathrm{He}}(\vec{\mathrm{e}}, e'd)$ reaction, the virtual photon emitted by the incoming electron transfers the energy ω and momentum $\mathbf{q}$ to the ^{3}He nucleus. The process is best studied by measuring its response as a function of the magnitude of its missing momentum, which is defined as the difference between the momentum transfer and the detected deuteron momentum, $p_m = |\mathbf{q} - \mathbf{p}_d|$; hence, p_m corresponds to the momentum of the recoiled proton.

The unpolarized $^3\mathrm{He}(e, e'd)$ process has been studied at Bates and NIKHEF facilities [4–7], yielding information on nucleon momentum distributions, isospin structure of the currents, FSI, and MEC. However, these measurements lacked the selective power of those experiments that exploit polarization. Only a handful of such measurements exist. The $^3\overrightarrow{\mathrm{He}}(\vec{\mathrm{e}}, e'p)pn$ and $^3\overrightarrow{\mathrm{He}}(\vec{\mathrm{e}}, e'p)d$ channels have been studied at NIKHEF [8,9] and Mainz [10,11], but no published data on the polarized $^3\overrightarrow{\mathrm{He}}(\vec{\mathrm{e}}, e'd)$ exist, chiefly due to the fact that previous experiments, though attempted, lacked present-day highly polarized beams and targets, which resulted in poor experimental figures-of-merit and prohibitive uncertainties.

It has been shown, both in the diagrammatic approach [12–14], as well as in independent full Faddeev calculations of the Hannover-Lisbon (H-L) [15–18] and the Bochum-Krakow (B-K) [19,20] groups, that the $^3\overrightarrow{\mathrm{He}}(\vec{\mathrm{e}}, e'd)$ reaction exhibits strong sensitivities to the subleading components of the ^{3}He ground-state wave function and, possibly, three-nucleon forces. Because of a particular isoscalar-isovector interference, this channel is also a unique source of information on the isospin structure of the electromagnetic current. It is the sensitivity brought about by the polarization degrees of freedom, augmented by the extended lever arm in p_m, that lends the present experiment its benchmark strength. Especially the extended kinematic coverage in p_m up to 270 MeV$/c$ represents a crucial advantage, because the calculations enumerated above indicate that the manifestations of various ^{3}He wave function components exhibit very different signatures as functions of p_m. Moreover, these p_m dependencies in each ^{3}He breakup channel appear to be rather distinct.

In the case of polarized beam and polarized target, the cross section for the $^3\overrightarrow{\mathrm{He}}(\vec{\mathrm{e}}, e'd)$ reaction has the form

$$\frac{d\sigma(h, \vec{S})}{d\Omega} = \frac{d\sigma_0}{d\Omega}[1 + \vec{S}\cdot\vec{A}^0 + h(A_e + \vec{S}\cdot\vec{A})],$$

where $d\Omega = d\Omega_e dE_e d\Omega_d$ is the differential of the phase-space volume, σ_0 is the unpolarized cross section, $\vec{S}$ is the spin of the target, and h is the helicity of the electrons. The $\vec{A}^0$ and A_e are the asymmetries induced by the polarization of only the target or only the beam, respectively, while the spin-correlation parameter $\vec{A}$ is the asymmetry when both the beam and the target are polarized. If the target is polarized only in the horizontal plane defined by the beam and scattered electron momenta (see Fig. 1), the term $\vec{S}\cdot\vec{A}^0$ does not contribute [12], while A_e is parity suppressed and is negligible with respect to $\vec{A}$.

The orientation of the target polarization is defined by the angles θ^* and ϕ^* in the frame where the z axis is along $\mathbf{q}$

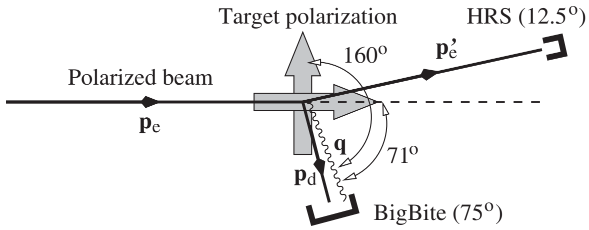

FIG. 1. Schematic drawing of the experimental setup. The orientations of the in-plane target polarization along the beam line and perpendicular to it correspond to the spherical angles about the $\mathbf{q}$ vector of $\theta^* = 71°$ and $\theta^* = 160°$, respectively, with $\phi^* = 0°$ in both cases.

and the y axis is given by $\mathbf{p}_e \times \mathbf{p}'_e$. Any component of $\vec{A}$, i.e., the asymmetry at given θ^* and ϕ^* is then

$$A(\theta^*, \phi^*) = \frac{(d\sigma/d\Omega)_+ - (d\sigma/d\Omega)_-}{(d\sigma/d\Omega)_+ + (d\sigma/d\Omega)_-}, \qquad (1)$$

where the subscript signs represent the beam helicities. In this Letter we report measurements of these asymmetries in the $^3\overrightarrow{\mathrm{He}}(\vec{\mathrm{e}}, e'd)p$ process in quasielastic kinematics at the average four-momentum transfer of $Q^2 = \mathbf{q}^2 - \omega^2 = 0.25(\mathrm{GeV}/c)^2$, performed during the E05-102 experiment at the Thomas Jefferson National Accelerator Facility in experimental Hall A [21].

We used an electron beam with an energy of 2.425 GeV and currents in excess of 10 μA. The beam was longitudinally polarized, with an average polarization of $P_e = (84.3 \pm 2.0)\%$ measured by a Møller polarimeter. The beam helicity was flipped at 30 Hz in $+--+$ or $-++-$ structures in pseudorandom sequence.

The beam was incident on a 40 cm-long glass target cell containing the ^{3}He gas at approximately 9.3 bar (corresponding to the surface-area density of 0.043 g/cm^2), which was polarized by hybrid spin-exchange optical pumping [22–25]. The in-plane orientation of the polarization was maintained by two pairs of Helmholtz coils. To measure the $A(160°, 0°)$ asymmetry, the coils were used to rotate the ^{3}He spin vector to the left of the beam, at 160° with respect to $\mathbf{q}$, while for the $A(71°, 0°)$ asymmetry it was maintained along the beam line, at 71° with respect to $\mathbf{q}$ (both values are averages over the whole spread of angles). Electron paramagnetic resonance and nuclear magnetic resonance [26–28] were used to monitor the polarization of the target, P_t, which was between 50% and 60% throughout the experiment and was taken into account on a run-by-run basis.

The scattered electrons were detected by a High-Resolution magnetic Spectrometer (HRS) positioned at $\theta_e = 12.5°$ and equipped with a detector package consisting of a pair of scintillator planes used for triggering and time-of-flight measurements, vertical drift chambers for particle tracking, and a gas Čerenkov counter and lead-glass calorimeters for particle identification.

The ejected deuterons and protons were detected by the large-acceptance spectrometer BigBite, equipped with a detector package optimized for hadron detection [29], consisting of a pair of multiwire drift chambers used for tracking and two scintillator planes used for triggering, time-of-flight determination, and particle identification.

The electrons in the HRS were selected by applying cuts on the Čerenkov detector signals. The most reliable selection of deuterons in BigBite was achieved by using graphical cuts in two-dimensional histograms of scintillator ADC (particle energy loss) vs particle momentum as determined from track reconstruction. Depending on the kinematics, (1–2)% of protons may become misidentified as deuterons, which has a minute influence on the final results. For the extraction of the asymmetries, only electron-deuteron coincidence events were retained, based on the measurement of coincidence time. Additional cuts on the location of the target vertex (to eliminate the contribution from the cell walls) and on the quality of the reconstructed tracks were used to further purify the event sample.

The experimental asymmetry for each orientation of the target polarization was determined as the relative difference between the number of coincidence events (after all cuts and background subtraction) corresponding to positive and negative beam helicities, $A_{\mathrm{exp}} = (N_+ - N_-)/(N_+ + N_-)$, where N_+ and N_- have been corrected for helicity-gated beam charge asymmetry, dead time, and radiative effects. The corresponding physics asymmetries were calculated as $A = A_{\mathrm{exp}}/(P_e P_t)$.

The asymmetries as functions of p_m are shown in Fig. 2. The largest contribution to the systematic error comes from the relative uncertainty of the target polarization, P_t, which has been estimated at 5%, followed by the uncertainty due to protons contaminating the deuteron sample, an effect that translates into a systematic error of 3% at low hadron momenta to less than 1% at high momenta. The absolute error of the beam polarization, P_e, was 2%, while the error due to the uncertainty of the target orientation angle θ^* was 0.6%. Because of finite spectrometer acceptances there was a spread in θ^* and ϕ^* around their nominal values, which has been taken into account in the theory acceptance-averaging procedure. The total systematic uncertainty (all items added in quadrature) is 7% (relative). The resolution in p_m is driven mostly by the relative momentum resolution of BigBite, which is ≈2% for all momenta [29], while the contribution of the ω resolution (2.2×10^{-4}) is negligible. Hence, the kinematic dependence of the systematic uncertainties is very small, and the possible smearing of the asymmetries has been excluded.

Figure 2 also shows the results of the state-of-the-art three-body calculations of the Hannover-Lisbon [15–18], Bochum-Krakow [19,20], and Pisa [30] groups. The B-K calculations are based on the AV18 nucleon-nucleon

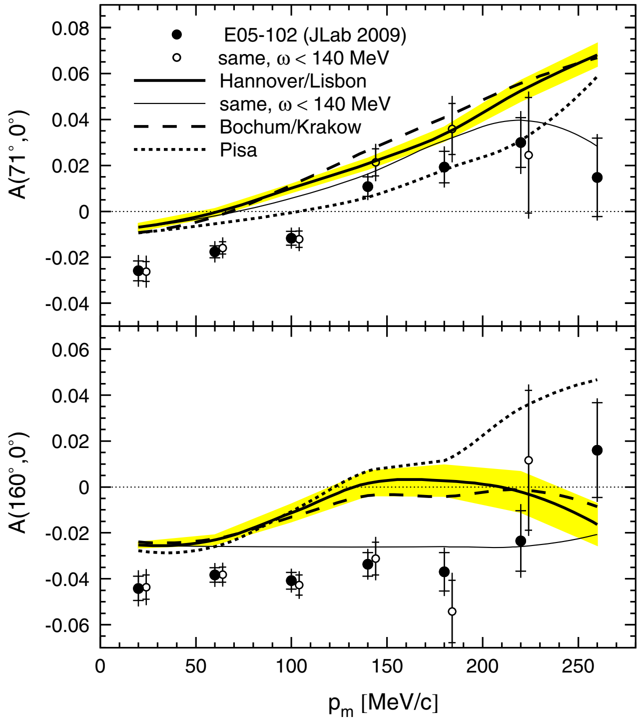

FIG. 2 (color online). The asymmetries $A(71°, 0°)$ (top) and $A(160°, 0°)$ (bottom) in the quasielastic $^3\overrightarrow{\mathrm{He}}(\vec{\mathrm{e}}, e'd)$ process as functions of missing momentum, compared to the acceptance-averaged calculations of the Hannover-Lisbon, Bochum-Krakow, and Pisa groups. The double error bars on the data denote the statistical and total uncertainties (statistical and systematical part added linearly). The shaded (yellow) bands indicate the uncertainties implied by the acceptance-averaging procedure. They have been placed on the H-L curves because that calculation has been averaged over the finest mesh. Empty symbols (shifted for clarity) and thin curves denote the data and the corresponding H-L calculation with a cut on the quasielastic peak.

potential [31,32] and involve a complete treatment of FSI and MEC, but do not include three-nucleon forces; the Coulomb interaction is taken into account in the ^{3}He bound state. The H-L calculations are based on the coupled-channel extension of the charge-dependent Bonn potential [33] and also include FSI and MEC, while the Δ isobar is added as an active degree of freedom providing a mechanism for an effective three-nucleon force and for exchange currents. Point Coulomb interaction is added in the partial waves involving two charged baryons. The Pisa calculations are based on the AV18 interaction model (augmented by the Urbana IX three-nucleon force [34]), in which full inclusion of FSI is taken into account by means of the variational pair-correlated hyperspherical harmonic expansion, as well as MEC. Coulomb interaction is included in full (not only in the ^{3}He ground state). In contrast to the B-K and H-L approaches, the Pisa calculations are not genuine Faddeev calculations but are of equivalent precision and are expected to account for all relevant reaction mechanisms.

Because of the extended momentum and angular acceptances of HRS and BigBite, the theoretical asymmetries were averaged over these acceptances. The averaging was performed over the whole accepted region of the (E'_e, θ_e) plane in 63 bins for the H-L calculations and 35 bins for the B-K and Pisa calculations. In each of these bins, the asymmetries were evaluated on a mesh of p_m and deuteron azimuthal angles with respect to $\mathbf{q}$, and interpolated. The acceptance-averaged theoretical asymmetries for each p_m bin and their errors originating in this procedure were then obtained by evaluating a weighted average and mapped onto the seven p_m bins used to display the measured asymmetries.

Neither of the three considered theories exactly reproduces the measured $A(160°, 0°)$ asymmetry—which is fairly constant at about −4% throughout the p_m range—except when a quasielastic cut ($\omega < 140$ MeV) is applied. The improved agreement is not surprising as all present calculations are known to perform better in the region of the quasielastic peak, while their reliability is expected to deteriorate in the dip region and beyond due to the opening of the pion production threshold and increasing influences of resonances, all of which have so far not been taken into account. A hint of the zero crossing of the measured asymmetry at high p_m appears to be mirrored by the theoretical one, but it occurs at much lower p_m, and the predicted asymmetries, in addition to exhibiting a mismatch in the functional form, are roughly a factor of 2 too small. On the other hand, the measured $A(71°, 0°)$ shows a clear zero crossing at $p_m \approx 130$ MeV/c seen also in all three calculations, although it again occurs at much lower p_m.

One could argue that, at low p_m, the asymmetries for the deuteron knock-out process $^3\overrightarrow{\mathrm{He}}(\vec{\mathrm{e}}, e'd)$ should be similar to the asymmetries for electron scattering almost elastically off a polarized deuteron within polarized ^{3}He. To assess this instructive, if simplistic, view we have equated the measured $A(160°, 0°)$ and $A(71°, 0°)$ for ^{3}He at low p_m ($p_m \leq 40$ MeV/c) with the corresponding $\vec{\mathrm{e}}$-$\vec{\mathrm{d}}$ asymmetries, computed at the same (θ^*, ϕ^*) and Q^2. By using appropriate deuteron form factors [35] one can extract the vector and tensor spin orientations of the deuteron, P_z and P_{zz}, inside ^{3}He. From the data, we obtain $P_z(\exp) = 0.72 \pm 0.11$ and $P_{zz}(\exp) = 0.82 \pm 0.14$, indicating—under the above assumptions—that the deuteron in ^{3}He is strongly polarized (spin-up), the third component of zero being disfavored due to $P_{zz} \approx 1$. By applying the same procedure on the theoretical predictions, we obtain P_z of 0.20–0.27 and P_{zz} of 0.95–1.01, depending on the model (see Fig. 3). In this approximation, the incomplete theoretical description of both $^3\overrightarrow{\mathrm{He}}(\vec{\mathrm{e}}, e'd)$ asymmetries at low p_m maps to an inadequacy in just one parameter, P_z, which is underestimated by a factor of about 3, while P_{zz} is only slightly overestimated.

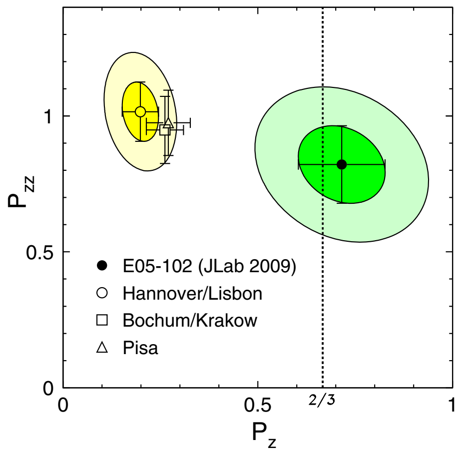

FIG. 3 (color online). Effective vector and tensor deuteron polarizations (spin orientations) P_z and P_{zz} in ^{3}He extracted from the data and theoretical predictions at $p_m \to 0$ in the approximation of e-d elastic scattering [with 1σ and 2σ covariance ellipses on the experiment (green) and the numerically most reliable theory interpolation (H-L, yellow)]. If the spin part of the ^{3}He wave function were given simply by a Clebsch-Gordan combination of the proton and deuteron parts, one would expect $P_z = 2/3$ and $P_{zz} = 0$.

The asymmetries as functions of energy transfer ω are shown in Fig. 4. At low ω, both measured asymmetries, $A(160°, 0°)$ and $A(71°, 0°)$, are fairly well reproduced in all approaches in terms of the functional form, but not in magnitude: again, there is a systematic offset of the asymmetries of about 1% or 2% (absolute). At high ω, all calculated asymmetries deviate from the measured ones, even in the H-L prediction that has been evaluated on the finest mesh, indicating that the dynamic input in the theoretical treatment of the process in the dip region is incomplete.

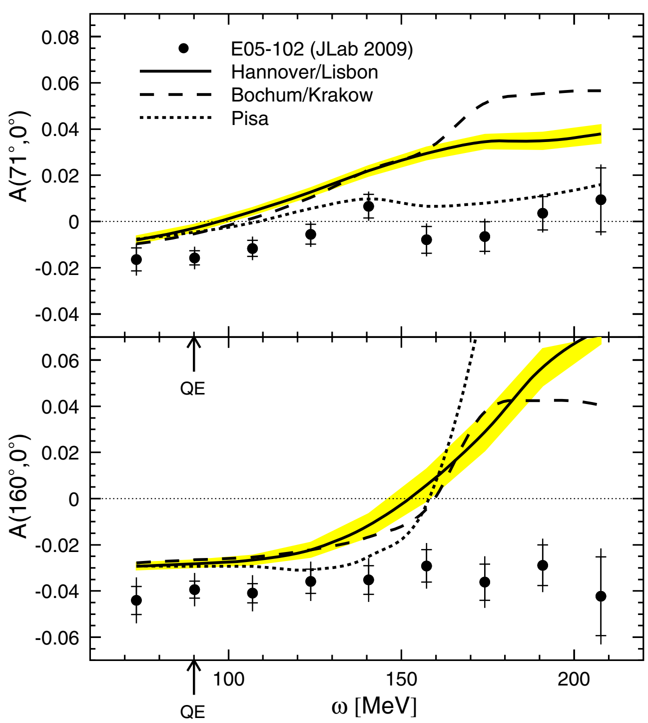

FIG. 4 (color online). The asymmetries $A(71°, 0°)$ and $A(160°, 0°)$ in the $^3\overrightarrow{\mathrm{He}}(\vec{e}, e'd)$ process as functions of energy transfer. The arrows denote the approximate location of the quasielastic peak.

In conclusion, we have provided the world-first, high-precision data on a high-level physics observable at two different spin settings in a broad kinematic range. Three most sophisticated theoretical treatments of the ^{3}He system are able to qualitatively account for the bulk of our data set; given the small magnitude of the asymmetries and the subtle interplay of the myriad of their ingredients, the agreement is actually quite good—in spite of the systematic offsets in p_m and ω dependencies and deviations occurring in the dip region. Up to the level of this agreement, the basic theoretical assumptions on the hadron dynamics and on the structure of the electromagnetic currents have been justified, and it appears that a consistent ^{3}He ground-state wave function has been employed. However, the large precision of our measurements has been able to reveal deficiencies in the calculations, indicating a need for further refinement in the treatment of their two-and/or three-body dynamics. In fact, the detailed anatomy of the p_m dependence of asymmetries is already the subject of a major ongoing theoretical effort. Among other things, our data will now allow one to check which leading and subleading components make up the employed ^{3}He wave function that are consistent with the assumed dynamics, and thereby significantly advance our knowledge of the three-nucleon system.

We thank the Jefferson Lab Hall A and Accelerator Operations technical staff for their outstanding support. This material is based upon work supported by the U.S. Department of Energy, Office of Science, Office of Nuclear Physics under Contract No. DE-AC05-06OR23177. This work was supported in part by the Polish National Science Center under Grant No. DEC-2013/10/M/ST2/00420. The numerical calculations of the Bochum-Krakow group were partly performed on the supercomputer cluster of the JSC, Jülich, Germany.

*Deceased.
†Present address: Institut für Kernphysik, Johannes-Gutenberg-Universität, Mainz, Germany.
‡Corresponding author.
simon.sirca@fmf.uni-lj.si

[1] W. Glöckle, J. Golak, R. Skibiński, H. Witała, H. Kamada, and A. Nogga, Eur. Phys. J. A **21**, 335 (2004).
[2] J. Golak, R. Skibiński, H. Witała, W. Glöckle, A. Nogga, and H. Kamada, Phys. Rep. **415**, 89 (2005).
[3] S. Širca, Few-Body Syst. **47**, 39 (2010).

[4] P. H. M. Keizer, P. C. Dunn, J. W. A. Den Herder, E. Jans, A. Kaarsgaarn, L. Lapikás, E. N. M. Quint, P. K. A. De Witt Huberts, H. Postma, and J. M. Laget, Phys. Lett. **157B**, 255 (1985).
[5] C. Tripp *et al.*, Phys. Rev. Lett. **76**, 885 (1996).
[6] C. M. Spaltro *et al.*, Phys. Rev. Lett. **81**, 2870 (1998).
[7] C. M. Spaltro *et al.*, Nucl. Phys. **A706**, 403 (2002).
[8] H. R. Poolman *et al.*, Phys. Rev. Lett. **84**, 3855 (2000).
[9] D. W. Higinbotham *et al.*, Nucl. Instrum. Methods Phys. Res., Sect. A **444**, 557 (2000).
[10] C. Carasco *et al.*, Phys. Lett. B **559**, 41 (2003).
[11] P. Achenbach *et al.*, Eur. Phys. J. A **25**, 177 (2005).
[12] J.-M. Laget, Phys. Lett. B **276**, 398 (1992).
[13] S. Nagorny and W. Turchinetz, Phys. Lett. B **389**, 429 (1996).
[14] S. Nagorny and W. Turchinetz, Phys. Lett. B **429**, 222 (1998).
[15] L. P. Yuan, K. Chmielewski, M. Oelsner, P. U. Sauer, and J. Adam, Phys. Rev. C **66**, 054004 (2002).
[16] A. Deltuva, L. P. Yuan, J. Adam, A. C. Fonseca, and P. U. Sauer, Phys. Rev. C **69**, 034004 (2004).
[17] A. Deltuva, L. P. Yuan, J. Adam, and P. U. Sauer, Phys. Rev. C **70**, 034004 (2004).
[18] A. Deltuva, A. C. Fonseca, and P. U. Sauer, Phys. Rev. C **71**, 054005 (2005).
[19] J. Golak, W. Glöckle, H. Kamada, H. Witała, R. Skibiński, and A. Nogga, Phys. Rev. C **65**, 064004 (2002).
[20] J. Golak, R. Skibiński, H. Witała, W. Glöckle, A. Nogga, and H. Kamada, Phys. Rev. C **72**, 054005 (2005).
[21] J. Alcorn *et al.*, Nucl. Instrum. Methods Phys. Res., Sect. A **522**, 294 (2004).
[22] T. G. Walker and W. Happer, Rev. Mod. Phys. **69**, 629 (1997).
[23] S. Appelt, A. Baranga, C. Erickson, M. Romalis, A. Young, and W. Happer, Phys. Rev. A **58**, 1412 (1998).
[24] E. Babcock, I. A. Nelson, S. Kadlecek, B. Driehuys, L. W. Anderson, F. W. Hersman, and T. G. Walker, Phys. Rev. Lett. **91**, 123003 (2003).
[25] J. Singh *et al.*, arXiv:1309.4004 [Phys. Rev. C (to be published)].
[26] A. Abragam, *Principles of Nuclear Magnetism* (Oxford University Press, New York, 1961).
[27] M. V. Romalis and G. D. Cates, Phys. Rev. A **58**, 3004 (1998).
[28] E. Babcock, I. A. Nelson, S. Kadlecek, and T. G. Walker, Phys. Rev. A **71**, 013414 (2005).
[29] M. Mihovilovič *et al.*, Nucl. Instrum. Methods Phys. Res., Sect. A **686**, 20 (2012).
[30] L. E. Marcucci, M. Viviani, R. Schiavilla, A. Kievsky, and S. Rosati, Phys. Rev. C **72**, 014001 (2005).
[31] R. B. Wiringa, V. G. J. Stoks, and R. Schiavilla, Phys. Rev. C **51**, 38 (1995).
[32] S. Veerasamy and W. N. Polyzou, Phys. Rev. C **84**, 034003 (2011).
[33] R. Machleidt, Phys. Rev. C **63**, 024001 (2001).
[34] B. S. Pudliner, V. R. Pandharipande, J. Carlson, and R. B. Wiringa, Phys. Rev. Lett. **74**, 4396 (1995).
[35] D. Abbott *et al.*, Eur. Phys. J. A **7**, 421 (2000).